Continuum Mech. Thermodyn. (2018) 30:127–144
https://doi.org/10.1007/s00161-017-0591-9

ORIGINAL ARTICLE

M. P. Ramos · C. Ribeiro · A. J. Soares

Modeling and analysis of time-dependent processes in a chemically reactive mixture

Received: 20 January 2017 / Accepted: 29 July 2017 / Published online: 14 August 2017

Abstract In this paper, we study the propagation of sound waves and the dynamics of local wave disturbances induced by spontaneous internal fluctuations in a reactive mixture. We consider a non-diffusive, non-heat conducting and non-viscous mixture described by an Eulerian set of evolution equations. The model is derived from the kinetic theory in a hydrodynamic regime of a fast chemical reaction. The reactive source terms are explicitly computed from the kinetic theory and are built in the model in a proper way. For both time-dependent problems, we first derive the appropriate dispersion relation, which retains the main effects of the chemical process, and then investigate the influence of the chemical reaction on the properties of interest in the problems studied here. We complete our study by developing a rather detailed analysis using the Hydrogen–Chlorine system as reference. Several numerical computations are included illustrating the behavior of the phase velocity and attenuation coefficient in a low-frequency regime and describing the spectrum of the eigenmodes in the small wavenumber limit.

Keywords Chemically reactive flows · Sound propagation · Flow instabilities · Eigenmodes

1 Introduction

The behavior of sound waves propagating in chemically reactive systems is of great relevance in various modern engineering problems, and therefore, this subject has scientific and commercial interests [1–3]. In particular, the coupling between the chemical kinetics and the sound propagation is important for measuring physical and chemical properties of fluids. The application of mathematical models to study the dynamics of such wave problems can be useful to improve the theoretical research on this field and to investigate the effects of the chemical reactions on sound properties of the reactive system. There exist several studies in this field, showing that the sound propagation in reactive mixtures can be strongly affected by the chemical reaction. Among others, we quote here Refs. [1,4–8]. However, in our opinion, other contributions at the level

Communicated by Andreas Öchsner.

M. P. Ramos
Departamento de Matemática e Aplicações, Universidade do Minho, Braga, Portugal
E-mail: mpr@math.uminho.pt

C. Ribeiro · A. J. Soares (✉)
Centro de Matemática, Universidade do Minho, Braga, Portugal
E-mail: ajsoares@math.uminho.pt

C. Ribeiro
E-mail: cribeiro@math.uminho.pt

of theoretical and modeling approaches should be of interest in order to deeply investigate the effects of the chemical kinetics on sound propagation within reactive systems.

Our contribution presented in this paper goes in this direction, and we exploit the potentialities of the kinetic theory to give a rather detailed description of the chemical effects on the sound properties. In fact, the kinetic theory extended to chemically reactive mixtures provides a robust microscopic model to describe reactive systems, starting from the molecular dynamics of the particles. The reactive source terms representing the chemical kinetics of the reactive system, and the forward and backward rate constants in particular, can be explicitly computed and incorporated in the mathematical model in a very natural way [9]. Moreover, these source terms retain many parameters connected to the chemical kinetics of the mixture and this represents a great advantage in the analysis.

Having these ideas in mind, we present in this paper a mathematical model and a detailed numerical analysis to investigate the propagation of sound waves in chemically reactive mixtures. The modeling and the analysis are also applied to study the propagation of infinitesimal disturbances induced by spontaneous internal fluctuations in the reactive mixture.

The starting point for the present investigation is the study initiated in paper [8], where the focus was on the effects of the reaction heat on time-dependent problems within a binary reactive mixture. The modeling proposed in Ref. [8] is here extended to a quaternary mixture with bimolecular reaction and then applied taking as reference the Hydrogen–Chlorine system when the reaction is specialized in $H_2 + Cl \rightleftharpoons HCl + H$. The complexity of a quaternary reactive mixture enriches the description but, at the same time, brings many additional complications at the modeling level. Nevertheless, with the help of computational resources, we were able to derive explicitly the dispersion relation, compute its solutions and evaluate the properties of interest in the sound propagation problem and dynamics of small disturbances.

The presentation of our results is organized as follows. In Sect. 2, we briefly describe the mathematical model, introducing the basic quantities and source terms, and providing the hydrodynamic equations. In Sect. 3, we furnish the linear framework, search for harmonic wave solutions and derive the corresponding dispersion relation. Sections 4 and 5 are devoted to the study of sound propagation and dynamics of small disturbances, respectively. Computations are presented and discussed in Sect. 6, with reference to the Hydrogen–Chlorine system. Finally, in Sect. 7 we present some concluding remarks.

2 Basic quantities and hydrodynamic model

In this section, we introduce the basic fields and the corresponding hydrodynamic equations for the description of the chemically reacting mixture. We consider a reactive mixture of monatomic gases with four constituents A_α, $\alpha = 1, \ldots, 4$, undergoing the reversible bimolecular reaction represented by

$$A_1 + A_2 \rightleftharpoons A_3 + A_4. \tag{1}$$

For each constituent A_α, we introduce the molecular diameter d_α, the formation (or binding) energy ϵ_α, and the molecular mass m_α. Due to the mass conservation during the chemical reaction (1), we have $m_1 + m_2 = m_3 + m_4 = M$.

2.1 Macroscopic basic fields

The basic fields of the reactive mixture are the mass densities ϱ_α of the constituents, $\alpha = 1, \ldots, 4$, the momentum density ϱv and the total energy density ϱe of the whole mixture, with $\varrho = \sum_{\alpha=1}^{4} \varrho_\alpha$, v and e being the mass density, mean velocity and total specific energy of the mixture.

Other fields of the mixture are the number density n_α of each constituent, the pressure p, number density n and temperature T of the mixture, with $n_\alpha = \varrho_\alpha / m_\alpha$ and $n = \sum_{\alpha=1}^{4} n_\alpha$.

The total energy density ϱe of the mixture is the sum of the internal energy and the kinetic energy, with the internal energy density $\varrho\varepsilon$ being, in turn, the sum of the thermal and binding energies, that is

$$\varrho e = \varrho\varepsilon + \frac{\varrho v^2}{2}, \qquad \varrho\varepsilon = \frac{3}{2} p + \sum_{\alpha=1}^{4} n_\alpha \epsilon_\alpha. \tag{2}$$

2.2 Modeling assumptions

For the present analysis, we will assume the following properties about the reactive mixture. The space evolution is one-dimensional depending on the space coordinate $x \in \mathbb{R}$, so that all mixture fields depend on $(t, x) \in \mathbb{R}_0^+ \times \mathbb{R}$. The evolution regime is Eulerian, and thus, the mixture is non-diffusive, non-heat conducting and non-viscous. The chemical reaction is assumed a fast process, so that the mixture is not faraway from the chemical equilibrium. Moreover, molecular degrees of freedom, like vibrational, rotational, electronic and nuclei, are not taken into account, so each constituent A_α has only one degree of internal energy specified by ϵ_α. The chemical reaction can be treated properly in terms of the formation energies ϵ_α, see [9], and the chemical kinetics of the model is based on a chemical potential with internal variables associated with the formation energy, only, that is

$$\mu_\alpha = \epsilon_\alpha + kT\left[\ln n_\alpha - \frac{3}{2}\ln T - \frac{9}{4}\ln\left(\frac{2\pi k m_\alpha}{h^2}\right)\right], \qquad \alpha = 1, \ldots, 4, \tag{3}$$

where k is the Boltzmann constant and h the Planck constant.

All constituents have equal specific heat ratios, that is $\gamma_\alpha = \gamma = 5/3$, for $\alpha = 1, \ldots, 4$. They also have specific heats at constant volume that are independent of the temperature,

$$c_{\mathrm{v}}^\alpha = \frac{k}{m_\alpha(\gamma - 1)}, \qquad \alpha = 1, \ldots, 4, \tag{4}$$

so that the constant volume specific heat of the mixture, defined by $c_{\mathrm{v}} = \frac{1}{\varrho}\sum_{\alpha=1}^4 \varrho_\alpha c_{\mathrm{v}}^\alpha$, can be written as

$$c_{\mathrm{v}} = \frac{3kn}{2\varrho}. \tag{5}$$

Furthermore, we assume that the mixture obeys the thermal equation of state,

$$p = nkT, \tag{6}$$

and thus the internal energy density $\varrho\varepsilon$ can be expressed in terms of the temperature T as

$$\varrho\varepsilon = \sum_{\alpha=1}^4 n_\alpha \epsilon_\alpha + \varrho c_{\mathrm{v}} T. \tag{7}$$

2.3 Model equations

The hydrodynamic equations of our model are those for an Eulerian reacting mixture, formed by the balance equations for the mass densities of the constituents and conservation equations for the momentum and total energy of the mixture. In one-space dimension form, such equations are given by

$$\frac{\partial \varrho_\alpha}{\partial t} + \frac{\partial}{\partial x}(\varrho_\alpha v) = \tau_\alpha, \qquad \alpha = 1, \ldots, 4, \tag{8}$$

$$\frac{\partial}{\partial t}(\varrho v) + \frac{\partial}{\partial x}(\varrho v^2 + p) = 0, \tag{9}$$

$$\frac{\partial}{\partial t}(\varrho e) + \frac{\partial}{\partial x}(\varrho e v + p v) = 0, \tag{10}$$

where τ_α represents the reaction rate of constituent A_α describing the interaction among the constituents due to the chemical reaction (1). The closure of Eqs. (8–10) is achieved when the reaction rates τ_α are specified, as explained below.

For the analysis developed in this paper, it is convenient to write the reactive Euler Eqs. (8–10) in matrix form, and we obtain

$$\frac{\partial \mathbf{U}}{\partial t} + \mathbf{A}(\mathbf{U})\frac{\partial \mathbf{U}}{\partial x} = \mathbf{S}(\mathbf{U}), \tag{11}$$

where $\mathbf{U}$ is the vector of the mixture fields, $\mathbf{U} = [u_1\ u_2\ u_3\ u_4\ u_5\ u_6]^{\mathrm{T}} = [\varrho_1\ \varrho_2\ \varrho_3\ \varrho_4\ \varrho v\ \varrho e]^{\mathrm{T}}$, and $\mathbf{S}(\mathbf{U})$ the vector of the source contributions, $\mathbf{S}(\mathbf{U}) = [\tau_1\ \tau_2\ \tau_3\ \tau_4\ 0\ 0]^{\mathrm{T}}$. Moreover, $\mathbf{A}(\mathbf{U})$ represents the Jacobian matrix of the Euler system whose nonzero entries are

$$
\begin{aligned}
&\mathbf{A}_{11} = \frac{v}{\varrho}\left(\varrho_2+\varrho_3+\varrho_4\right), && \mathbf{A}_{12} = \mathbf{A}_{13} = \mathbf{A}_{14} = -\frac{\varrho_1 v}{\varrho}, && \mathbf{A}_{15} = \frac{\varrho_1}{\varrho},\\
&\mathbf{A}_{21} = \mathbf{A}_{23} = \mathbf{A}_{24} = -\frac{\varrho_2 v}{\varrho}, && \mathbf{A}_{22} = \frac{v}{\varrho}\left(\varrho_1+\varrho_3+\varrho_4\right), && \mathbf{A}_{25} = \frac{\varrho_2}{\varrho},\\
&\mathbf{A}_{31} = \mathbf{A}_{32} = \mathbf{A}_{34} - \frac{\varrho_3 v}{\varrho}, && \mathbf{A}_{33} = \frac{v}{\varrho}\left(\varrho_1+\varrho_2+\varrho_4\right), && \mathbf{A}_{35} = \frac{\varrho_3}{\varrho},\\
&\mathbf{A}_{41} = \mathbf{A}_{42} = \mathbf{A}_{43} = -\frac{\varrho_4 v}{\varrho}, && \mathbf{A}_{44} = \frac{v}{\varrho}\left(\varrho_1+\varrho_2+\varrho_3\right), && \mathbf{A}_{45} = \frac{\varrho_4}{\varrho},\\
&\mathbf{A}_{5\alpha} = -\frac{2}{3}\left(v^2+\frac{\epsilon_\alpha}{m_\alpha}\right)+g_\alpha, && \mathbf{A}_{55} = \frac{4}{3}v, && \mathbf{A}_{56} = \frac{2}{3},\\
&\mathbf{A}_{6\alpha} = \frac{v}{\varrho}\left(g_\alpha+\frac{2}{3}h_\alpha\right)-ev-\frac{pv}{\varrho}, && \mathbf{A}_{65} = e+\frac{p}{\varrho}-\frac{2}{3}v^2, && \mathbf{A}_{66} = \frac{5}{3}v,
\end{aligned}
\tag{12}
$$

where $g_\alpha = \frac{kT}{\varrho}\left(\frac{\varrho}{m_\alpha}-n\right)$, $h_\alpha = \frac{v^2}{2}-\frac{\epsilon_\alpha}{m_\alpha}$, for $\alpha = 1,\ldots,4$.

2.4 Chemical reaction rates

In our analysis, the reaction rates τ_α appearing in Eq. (8) are obtained from the kinetic theory of reactive mixtures, assuming reactive differential cross sections with activation energy and a particular form of the velocity distribution function that results to be appropriate for the considered Eulerian regime (see, for example, Ref. [9]). Following a standard procedure in kinetic theory, the reaction rates τ_α were explicitly evaluated in the form of an Arrhenius law as

$$
\tau_\alpha = -\nu_\alpha m_\alpha\Big[k_{34}(T)n_3n_4 - k_{12}(T)n_1n_2\Big], \qquad \nu_1=\nu_2=-\nu_3=-\nu_4=-1, \tag{13}
$$

where ν_α is the stoichiometric coefficient of each constituent, and $k_{34}(T)$, $k_{12}(T)$ denote the forward and reverse reaction rate coefficients given by

$$
k_{12}(T) = \sqrt{\frac{8\pi kT}{m_{12}}}d_{\mathrm{f}}^2\,\exp\!\Big(-\frac{\epsilon_{\mathrm{f}}}{kT}\Big), \qquad k_{34}(T) = \sqrt{\frac{8\pi kT}{m_{34}}}d_{\mathrm{r}}^2\,\exp\!\Big(-\frac{\epsilon_{\mathrm{r}}}{kT}\Big). \tag{14}
$$

Here, $\epsilon_{\mathrm{f}} = \epsilon_3+\epsilon_4$, $\epsilon_{\mathrm{r}} = \epsilon_1+\epsilon_2$ are the forward and backward activation energies, $Q = \epsilon_{\mathrm{f}}-\epsilon_{\mathrm{r}}$ is the reaction heat, $m_{12} = m_1m_2/M$, $m_{34} = m_3m_4/M$ are reduced masses of reactants and products, and d_{f}, d_{r} represent the reactive diameters in the forward and backward reactions, with $d_{\mathrm{f}} = d_{12}s_{\mathrm{f}}$, where $s_{\mathrm{f}} \in [0,1]$ is the steric factor of the forward reaction, $d_{12} = \frac{1}{2}(d_1+d_2)$, and $d_{\mathrm{r}} = \sqrt{m_{12}/m_{34}}\,d_{\mathrm{f}}$. Note that, for each α, the number density n_α of the constituent A_α represents a measure of the constituent's concentration in the mixture.

2.5 Chemical equilibrium

The reactive mixture reaches the chemical equilibrium if the reaction rates τ_α vanish. Thus, from expressions (13), we obtain the equilibrium condition

$$
\frac{n_1^{\mathrm{eq}}n_2^{\mathrm{eq}}}{n_3^{\mathrm{eq}}n_4^{\mathrm{eq}}} = \left(\frac{m_1m_2}{m_3m_4}\right)^{3/2}\exp\left(\frac{Q}{kT}\right), \tag{15}
$$

which represents the *mass action law* of our model and gives a constraint on the equilibrium number densities n_α^{eq}, temperature T of the mixture, molecular masses m_α of the constituents and reaction heat Q.

We conclude this section by emphasizing that our mathematical model for the analysis developed in the following sections is based on Eq. (11), with the source contributions defined by expression (13).

3 Linear analysis and dispersion relation of normal modes

Starting from the mathematical modeling described in the previous section, we study here the dynamics of small amplitude propagating waves in a chemically reactive mixture. As usual, we assume that the perturbations of the macroscopic fields have small amplitudes. Therefore, the state variables slightly deviate from the equilibrium and a linear theory results to be appropriate in describing the dynamics of the perturbations induced on the hydrodynamic fields.

Accordingly, we linearize the reactive Euler equations (11) around an equilibrium state characterized by a vanishing velocity, $v = 0$, and constant values of both the mass densities of the constituents, ϱ_α^0, and the total specific energy of the mixture, $\varrho_0 e_0 = \varrho_0 \varepsilon_0$. For such an equilibrium state, the reaction rate vanishes, τ_α^0, and the chemical equilibrium condition (15) holds true.

We then expand the state vector $\mathbf{U}$ in the form

$$\mathbf{U} = \mathbf{U}_0 + \overline{\mathbf{U}}, \tag{16}$$

where $\mathbf{U}_0$ stands for the equilibrium state and $\overline{\mathbf{U}}$ represents the vector of the perturbations, given by

$$\mathbf{U}_0 = \left[\, \varrho_1^0 \;\varrho_2^0 \;\varrho_3^0 \;\varrho_4^0 \;0 \;(\varrho\, e)^0 \,\right]^{\mathrm{T}}, \quad \overline{\mathbf{U}} = \left[\, \bar{u}_1 \;\bar{u}_2 \;\bar{u}_3 \;\bar{u}_4 \;\bar{u}_5 \;\bar{u}_6 \,\right]^{\mathrm{T}}. \tag{17}$$

3.1 Linearized field equations

Considering expansion (16) of the state vector $\mathbf{U}$ and the consequent expansions induced on the Jacobian matrix $\mathbf{A}(\mathbf{U})$ and source contributions $\mathbf{S}(\mathbf{U})$, the reactive Euler Eq. (11) become

$$\frac{\partial \overline{\mathbf{U}}}{\partial t} + \mathbf{A}(\mathbf{U}_0)\,\frac{\partial \overline{\mathbf{U}}}{\partial x} = \left(\frac{\partial \mathbf{S}}{\partial \mathbf{U}}\right)_0 \overline{\mathbf{U}}, \tag{18}$$

where we have disregarded all nonlinear terms in the perturbations and taken into account that the source contributions vanish at equilibrium, *i.e.,* $\mathbf{S}(\mathbf{U}_0) = 0$. Furthermore, the terms $\mathbf{A}(\mathbf{U}_0)$ and $\left(\frac{\partial \mathbf{S}}{\partial \mathbf{U}}\right)_0$ represent the matrix $\mathbf{A}$ and the Jacobian matrix of the source terms evaluated at the equilibrium state. The nonzero entries of the matrix $\mathbf{A}(\mathbf{U}_0) = \left(\mathbf{A}^0_{\alpha\beta}\right)$, $\alpha, \beta = 1, ..., 6$, are given by

$$\begin{aligned}
&\mathbf{A}^0_{\alpha 5} = \frac{\varrho^0_\alpha}{\varrho_0}, \quad \alpha = 1, \ldots, 4, && \mathbf{A}^0_{65} = e_0 + \frac{p_0}{\varrho_0},\\
&\mathbf{A}^0_{5\beta} = -\frac{2}{3}\frac{\epsilon_\beta}{m_\beta} + \frac{p_0}{\varrho_0}\left(\frac{\varrho_0}{m_\beta n_0} - 1\right), \quad \beta = 1, \ldots, 4, && \mathbf{A}^0_{56} = \frac{2}{3},
\end{aligned} \tag{19}$$

and the nonzero entries of the matrix $\left(\frac{\partial \mathbf{S}}{\partial \mathbf{U}}\right)_0 = \left(\mathbf{H}_{\alpha\beta}\right)$ are given by

$$\begin{aligned}
\mathbf{H}_{\alpha\alpha} &= -\frac{\Delta}{\tau x^{\mathrm{eq}}_\alpha} + m_\alpha\left(\frac{n}{\varrho} + \frac{2}{3m_\alpha}\frac{\epsilon_\alpha}{kT}\right) Q^*\frac{\Delta}{\tau}\,,\\
\mathbf{H}_{\gamma\gamma} &= -\frac{\Delta}{\tau x^{\mathrm{eq}}_\gamma} - m_\gamma\left(\frac{n}{\varrho} + \frac{2}{3m_\gamma}\frac{\epsilon_\gamma}{kT}\right) Q^*\frac{\Delta}{\tau}\,,\\
\mathbf{H}_{\alpha\beta} &= -\frac{m_\alpha}{m_\beta}\frac{\Delta}{\tau x^{\mathrm{eq}}_\beta} + m_\alpha\left(\frac{n}{\varrho} + \frac{2}{3m_\beta}\frac{\epsilon_\beta}{kT}\right) Q^*\frac{\Delta}{\tau}, \quad \alpha \neq \beta,\\
\mathbf{H}_{\alpha\gamma} &= \frac{m_\alpha}{m_\gamma}\frac{\Delta}{\tau x^{\mathrm{eq}}_\gamma} + m_\alpha\left(\frac{n}{\varrho} + \frac{2}{3m_\gamma}\frac{\epsilon_\gamma}{kT}\right) Q^*\frac{\Delta}{\tau},\\
\mathbf{H}_{\gamma\alpha} &= \frac{m_\gamma}{m_\alpha}\frac{\Delta}{\tau x^{\mathrm{eq}}_\alpha} - m_\gamma\left(\frac{n}{\varrho} + \frac{2}{3m_\alpha}\frac{\epsilon_\alpha}{kT}\right) Q^*\frac{\Delta}{\tau},\\
\mathbf{H}_{\gamma\delta} &= -\frac{m_\gamma}{m_\delta}\frac{\Delta}{\tau x^{\mathrm{eq}}_\delta} - m_\gamma\left(\frac{n}{\varrho} + \frac{2}{3m_\delta}\frac{\epsilon_\delta}{kT}\right) Q^*\frac{\Delta}{\tau}, \quad \gamma \neq \delta,\\
\mathbf{H}_{\alpha 6} &= -\frac{2}{3}\frac{m_\alpha}{kT} Q^*\frac{\Delta}{\tau}, \qquad \mathbf{H}_{\gamma 6} = \frac{2}{3}\frac{m_\gamma}{kT} Q^*\frac{\Delta}{\tau},
\end{aligned} \tag{20}$$

with $\alpha, \beta = 1, 2$ and $\gamma, \delta = 3, 4$. Here we have introduced the concentration of each constituent, $x_\alpha^{\text{eq}} = n_\alpha^{\text{eq}}/n$, for $\alpha = 1, \ldots, 4$, the dimensionless reaction heat, $Q^* = \frac{Q}{kT}$, and also the reference time τ and the pre-exponential Arrhenius factor Δ defined by

$$\tau = \frac{1}{4nd_{12}^2}\sqrt{\frac{m_{12}}{\pi kT}}\,, \quad \Delta = x_1^{\text{eq}} x_2^{\text{eq}} \frac{s_{\text{f}}^2}{\sqrt{2}} \exp\left(-\frac{\epsilon_{\text{f}}}{kT}\right). \tag{21}$$

The details of the calculations for the components of the first line of matrix $\mathbf{H}$ are given in Appendix.

3.2 Plane harmonic waves

Considering that the perturbation waves described by system (18) are plane harmonic waves with angular frequency ω and wavenumber κ, traveling in the x-direction, we look for solutions to system (18) of the form

$$\overline{\mathbf{U}} = \widetilde{\mathbf{U}} \exp\left[\imath\,(\kappa x - \omega t)\right], \tag{22}$$

where $\widetilde{\mathbf{U}}$ is the vector of small amplitudes of the harmonic waves, whose components are complex constants. By inserting the wave expansions (22) into the linear differential equations (18), we obtain the following homogeneous linear algebraic system for the wave amplitudes,

$$\Big(\omega\mathbf{I} - \kappa\mathbf{A}(\mathbf{U}_0) - \imath\mathbf{H}(\mathbf{U}_0)\Big)\widetilde{\mathbf{U}} = 0, \tag{23}$$

where $\mathbf{I}$ is the identity matrix of order six. Non-trivial solutions to system (23) follow when

$$\det\Big(\omega\mathbf{I} - \kappa\mathbf{A}(\mathbf{U}_0) - \imath\mathbf{H}(\mathbf{U}_0)\Big) = 0, \tag{24}$$

which defines the dispersion relation of the plane harmonic wave solutions (22) and enables us to determine the phase velocity and the attenuation coefficient of the waves.

In order to analyze the influence of the chemical reaction on the harmonic wave solutions, we also derive the dispersion relation of a non-reacting mixture. When we turn off the chemical reaction from our mixture, the corresponding dispersion relation can be explicitly computed from Eq. (24), giving rise to the following equation

$$\omega^4\left[\omega^2 - \frac{2}{3}\kappa^2\left(\varepsilon + \frac{p}{\varrho} + \frac{1}{\varrho}\sum_{\alpha=1}^{4} n_\alpha \epsilon_\alpha\right)\right] = 0, \tag{25}$$

where the symbols have the same meaning as before. The dispersion relations (24) and (25) constitute the key ingredients to investigate the sound wave propagation and the dynamics of local disturbances (eigenmodes) in the reactive mixture. This will be the object of our analysis in the next sections.

4 Sound wave propagation

In this section, we study the problem concerning the propagation of sound waves in the reactive mixture, in view of characterizing the effects of the chemical reaction in the relevant properties of the waves. We consider a propagation regime for which the sound frequency is significantly low. The sound wave problem can then be studied using the macroscopic equations of the previous sections, assuming that the perturbations induced by the sound propagation on the field variables are described by plane harmonic waves of type (22).

Due to the complexity of the problem and to the large amount of parameters characterizing the quaternary reactive mixture, we solve this problem for a specific quaternary mixture, following the steps presented in the sequel.

4.1 Formulation of the problem for sound waves

The problem of sound waves corresponds to the propagation of forced waves and consists in assuming a given real angular frequency ω and solving the dispersion relation (24) for a complex wavenumber κ as function of the oscillation frequency, that is $\kappa = \kappa(\omega)$. Then, the phase velocity and the attenuation coefficient of the waves can be computed from the roots of the dispersion relation, following a rather standard procedure (see, for example, [7,10–15]).

Accordingly, we write the wavenumber in the form $\kappa = \kappa_{\rm r} + \imath\kappa_{\rm i}$, where $\kappa_{\rm r} = Re(\kappa)$ and $\kappa_{\rm i} = {\rm Im}(\kappa)$ represent the real and imaginary parts of κ, so that the properties of interest for the sound propagation are obtained as the phase velocity $\boldsymbol{v}_{\rm p}$ and attenuation coefficient $\boldsymbol{\alpha}$ of the waves, given by

$$\boldsymbol{v}_{\rm p} = \frac{\omega}{\kappa_{\rm r}}, \qquad \boldsymbol{\alpha} = \kappa_{\rm i}. \tag{26}$$

Our aim is to analyze how the chemical reaction affects these properties, in particular how they are influenced by some of the parameters inherent to the chemical kinetics of the model.

4.2 Sound wave solutions

First, when considering a non-reacting mixture, we evaluate the corresponding phase velocity $\boldsymbol{v}_{\rm p*}$ and attenuation coefficient $\boldsymbol{\alpha}_*$ from the solutions to the dispersions relation (25) as

$$\boldsymbol{v}_{\rm p*} = \pm\sqrt{\frac{2}{3}\left[\varepsilon + \frac{p}{\varrho} - \frac{1}{\varrho}\sum_{\alpha=1}^{4} n_\alpha \epsilon_\alpha\right]} = \pm\sqrt{\frac{5}{3}\frac{p}{\varrho}} = \pm c\,, \qquad \boldsymbol{\alpha}_* = 0. \tag{27}$$

Expressions (27) reveal a well-known result for a non-reacting mixture of Eulerian gases [1,9,16] showing that, in absence of chemical reaction, as expected, the attenuation coefficient vanishes, whereas the phase velocity is independent of ω and κ and reduces to the sound speed $\pm c$ of a single monatomic gas. Therefore, there is no dispersion and no attenuation in the sound waves, and this can be justified by the fact that the transport coefficients are not taken into account and the chemical reaction is turned off.

Now we want to determine the solutions $\kappa = \kappa(\omega)$ to the dispersion relation (24) for the reactive mixture and then to evaluate the dimensionless reciprocal phase velocity $c/\boldsymbol{v}_{\rm p}$ and the dimensionless attenuation coefficient $\boldsymbol{\alpha}c/\omega$. Our aim is to analyze how the chemical reaction affects these properties, in particular how they are influenced by the activation energy of the chemical reaction and how they vary depending on the mixture temperature and constituent concentrations. To this end, we introduce the dimensionless wavenumber $\Gamma = \kappa c/\omega$ and the dimensionless oscillation frequency $\omega\tau$, with τ being the reference time given in (21). Then, we rewrite the dispersion relation (24) in terms of $\omega\tau$ and Γ, obtaining

$$\det\left[(\omega\tau)\left(\mathbf{I} - \frac{\Gamma}{c}\mathbf{A}(\mathbf{U}_0)\right) - \imath\tau\mathbf{H}(\mathbf{U}_0)\right] = 0, \tag{28}$$

and solve this equation for Γ as function of $\omega\tau$. Equation (28) determines an algebraic constraint between Γ and $\omega\tau$, which results in a polynomial equation of sixth degree in $\omega\tau$ and second degree in Γ, whose coefficients depend on the reaction heat Q^*, concentrations $x_\alpha^{\rm eq}$ and molecular masses m_α of the constituents, mixture temperature T, and activation energy $\epsilon_{\rm f}$ [through the Arrhenius factor Δ, see expression $(21)_2$]. Such polynomial equation is a huge and complicated equation, and it is not reasonable to write it here. The dispersion relation (28) reflects the influence of the chemical reaction and indicates that the model is able to capture the effects of the reactive process on the macroscopic fields variations due to the passage of sound waves.

The solutions Γ to the dispersion relation determine two propagating modes, for which the phase velocity and attenuation coefficient, are given by

$$\boldsymbol{v}_{\rm p}(\omega) = \frac{c}{\Gamma_{\rm r}}, \qquad \boldsymbol{\alpha}(\omega) = \frac{\omega\Gamma_{\rm i}}{c}, \tag{29}$$

where $\Gamma_{\rm r}$ and $\Gamma_{\rm i}$ are the real and imaginary parts of Γ.

Starting from the analysis developed in this section, and in particular from the dispersion relation (28) and its solutions Γ, detailed calculations can be performed once a particular mixture and associated chemical

reaction are specified. In Sect. 6, results are provided for different study cases for the Hydrogen–Chlorine system in which the elementary reaction $H_2 + Cl \rightleftharpoons HCl + H$ takes place. Several aspects regarding the influence of the chemical reaction on the sound propagation are presented and discussed.

5 Dynamics of local disturbances in the reactive mixture

In this section, we study the dynamics of local wave disturbances induced by spontaneous internal fluctuations in the reactive mixture. Our main objective is to characterize the propagating modes (eigenmodes) and investigate the influence of the chemical reaction on the parameters of interest in the process. We assume that the disturbances induced on the macroscopic fields are weak, and we are interested in the small wavenumber limit. The problem can then be well described using the linearized equations derived in Sect. 3, assuming that the disturbances are plane harmonic waves of type (22). In order to solve this problem, we follow the procedure explained below and perform a detailed numerical analysis to determine the solutions in a convenient parameter space.

5.1 Formulation of the problem of local wave disturbances

The problem of local wave disturbances corresponds to the propagation of free oscillations that decay in time, and is studied by assuming a given real wavenumber κ and solving the dispersion relation (24) for a complex angular frequency ω as function of the wavenumber, $\omega = \omega(\kappa)$. The oscillation frequency and the oscillation time decay of the disturbances can be computed from the roots of the dispersion relation, following a rather well-known procedure (see, for example, Refs. [7,17,18]).

We write the angular frequency as $\omega = \omega_\mathrm{r} + \imath\,\omega_\mathrm{i}$, with ω_r and ω_i being the real and imaginary parts of ω. Then, we determine the relevant properties of this problem, namely the oscillation frequency $\boldsymbol{\varphi}$ of the wave disturbances and the decay in time of their amplitude $\boldsymbol{\lambda}$, defined by

$$\boldsymbol{\varphi} = \omega_\mathrm{r}, \qquad \boldsymbol{\lambda} = \omega_\mathrm{i}. \tag{30}$$

Our goal is to characterize the spectrum of the eigenmodes for the considered reactive mixture and its dependence on the parameters connected to the chemical reaction.

5.2 Eigenmodes

First we derive the solutions to the dispersion relation (25) for a non-reacting mixture and obtain

$$\omega_{1,2,3,4} = 0 \qquad \text{and} \qquad \omega_5 = -\kappa c, \quad \omega_6 = +\kappa c, \tag{31}$$

which define four non-propagating eigenmodes and two propagating eigenmodes with symmetric real parts and zero imaginary parts. Solutions ω_5 and ω_6 describe hydrodynamic modes, since $\omega(\kappa) \to 0$ as $\kappa \to 0$, representing sound waves propagating in opposite directions with the same velocity (symmetric real parts) and no damping (zero imaginary parts).

In order to determine the spectrum of the eigenmodes of the reactive mixture, we use the dispersion relation (24) as explained before. Then, we introduce a reference length $\ell = \tau c$, with τ being the reference time defined in (21) and c the sound speed of the mixture, and rewrite the dispersion relation (24) in terms of the dimensionless oscillation frequency $\omega\tau$ and dimensionless wavenumber $\kappa\ell$. We obtain a rather cumbersome equation, due to the mathematical structure of the equations and source terms, which cannot be reproduced here. Its general form results in a polynomial equation of sixth degree in $\omega\tau$ and second degree in $\kappa\ell$, whose coefficients depend on Q^*, x_α^{eq}, m_α, T and ϵ_f. The corresponding solutions characterize the full spectrum of the eigenmodes for the considered reacting mixture, in particular they identify six eigenmodes classified in hydrodynamic modes and kinetic modes. See Refs. [7,17] for other details on the topic. The solutions also allow us to recognize the effects of the chemical reaction on the spectrum. However, in the small wavenumber limit, the solutions to the dispersion relation can be determined explicitly by expanding the dimensionless angular frequency $\omega\tau$ in power series of the dimensionless wavenumber $\kappa\ell$,

$$\omega\tau = b_0 + b_1(\kappa\ell) + b_2(\kappa\ell)^2 + \cdots, \tag{32}$$

and then looking for the complex expansion parameters $b_0,\ b_1,\ b_2, \ldots$

In the case of a generic quaternary reactive mixture, the dispersion relation is unmanageable from the analytical point of view, so our strategy is as follows. First we consider a specific reactive mixture and an elementary chemical reaction. Then, for any frequency regime, we derive the exact dispersion relation of the mixture and determine its solutions in view of characterizing the full spectrum of the eigenmodes. Finally, we focus on the small wavenumber limit and obtain an explicit representation of the solutions in the form of power series (32) and a detailed characterization of the eigenmodes.

Following this strategy, we consider in Sect. 6 the Hydrogen–Chlorine system and the elementary reaction $H_2 + Cl \rightleftharpoons HCl + H$. We give a rather detailed characterization of the eigenmodes and investigate the effects of the chemical reaction on the dynamics of the local disturbances. Numerical computations are presented and discussed.

6 Analysis of forced and free waves propagation

In this section, we perform a rather detailed analysis of forced and free waves, in view of studying the problems described in Sects. 4 and 5 and implementing the methodologies explained there. The formal theory presented in these sections is derived from the model described in Sect. 2, and there are some model parameters that play an important role in the chemical kinetics of the reactive mixture, like the molecular masses, activation energy and concentrations of the species, so our idea is to conduct a parametric study in order to investigate the influence of these parameters in the propagation of forced and free waves. Even if the formal theory is based in a model for monatomic mixtures, the data for our parametric study is taken from the Hydrogen–Chlorine system which is a polyatomic mixture. This represents a shortcoming of our analysis. However, at least from a qualitative point of view, our computations can provide general ideas about the role of the chemistry on both propagation problems. Accordingly, we consider three different mixtures of the Hydrogen–Chlorine system in which the elementary reaction $H_2 + Cl \rightleftharpoons HCl + H$ takes place. In Table 1, we present the mixtures, represented by $\mathcal{M}_i$, $i = 1, 2, 3$, indicating the concentrations of the constituents. In Table 2, we indicate the values of the molecular masses, molecular diameters and binding energies of the constituents at the temperature $T = 298.15$ K.

The analysis performed in this section addresses the problem of investigating the influence of the chemical reaction in the relevant properties of both processes. In order to better appreciate the chemical effects, we take $s_f = 1$ in all simulations implemented in this section. The computations are performed with the software *Maple*, version 12, for the considered mixtures, and the results are presented in Sects. 6.1 and 6.2.

The equilibrium concentrations x_α^{eq} and the molecular masses m_α reported in Tables 1 and 2 are constrained to the mass action law (15). Therefore, we evaluate the reaction heat at chemical equilibrium as a measure of the exothermicity or endothermicity degree of the reaction and obtain

$$Q^* = \frac{3}{2}\ln\left(\frac{m_3 m_4}{m_1 m_2}\right) + \ln\left(\frac{x_1^{eq} x_2^{eq}}{x_3^{eq} x_4^{eq}}\right). \tag{33}$$

Table 1 Reacting mixtures of the Hydrogen–Chlorine system

Reacting mixture	x_1^{eq}	x_2^{eq}	x_3^{eq}	x_4^{eq}
$\mathcal{M}_1$	0.20	0.20	0.30	0.30
$\mathcal{M}_2$	0.40	0.40	0.10	0.10
$\mathcal{M}_3$	0.25	0.25	0.25	0.25

Concentrations of the constituents

Table 2 Parameters characterizing the constituents

Constituent	Mass m_α ($\times 10^{-26}$ kg)	Diameter d_α ($\times 10^{-10}$ m)	Binding energy ϵ_α (kJ/mol)
H_2 (A_1)	0.335	2.90	0
Cl (A_2)	5.886	1.90	121.68
HCl (A_3)	6.054	3.30	−92.31
H (A_4)	0.167	1.50	217.97

and conclude that the chemical reaction is exothermic ($Q^* < 0$) for the mixtures $\mathcal{M}_1$ and $\mathcal{M}_3$, whereas it is endothermic ($Q^* > 0$) for the mixture $\mathcal{M}_2$.

6.1 Results for the sound propagation

In this subsection, we study the sound wave propagation in the low-frequency regime. In detail, we solve analytically the dispersion relation and determine the nonzero solutions for $\Gamma = \Gamma_\mathrm{r} + \imath\,\Gamma_\mathrm{i}$, specifying both the dimensionless reciprocal phase velocity and the attenuation coefficient through the relations $\Gamma_\mathrm{r}(\omega) = c/\boldsymbol{v}_\mathrm{p}(\omega)$ and $\Gamma_\mathrm{i}(\omega) = c\,\boldsymbol{\alpha}(\omega)/\omega$, see Eq. (29). In our study, only the effects of the chemical reaction on the sound properties are considered since transport effects and molecular degrees of freedom are not taken into account.

The results are shown in Figs. 1, 2 and 3, in the range $\omega \leq 2$GHz, where, for simplicity, we have used the notation ω for the dimensionless frequency $\omega\tau$. Left plots show the reciprocal phase velocity $c/\boldsymbol{v}_\mathrm{p}$ versus ω, and right plots show the attenuation coefficient $\boldsymbol{\alpha}c/\omega$ versus ω.

- The diagrams show, in general, that the chemical reaction contributes to decrease the phase velocity and increase the attenuation coefficient. This result is consistent with other papers studying sound propagation on chemically reactive mixtures (see, for example, [5,6]). However, in those papers, also the transport coefficients were included in the description, showing that the chemical reaction contributes to decrease the transport coefficients, and thus, the comparison is not straightforward.
- The deviations induced on both properties of the sound waves are more pronounced in the very low-frequency limit, *i.e.,* when $\omega \to 0$. The reciprocal phase velocity starts from a positive constant greater than 1, and then, decreases and asymptotically approximates the unity for increasing ω showing that the reactive phase velocity approaches the sound speed c of the inert mixture. The attenuation coefficient also shows a standard qualitative behavior (see [5,6,13,14]), starting from a very small value in the very low-frequency regime $\omega \to 0$, then increasing until a certain value of ω always less than 0.5, and then decreasing showing that the sound waves asymptotically tend to attenuate.

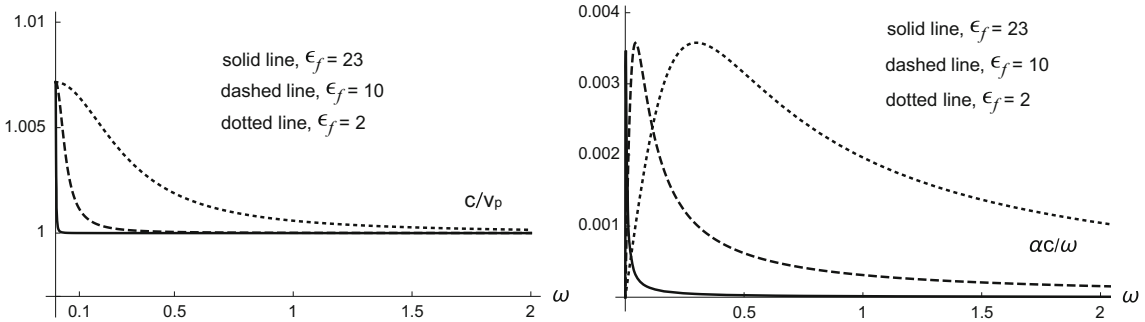

Fig. 1 Influence of the forward activation energy ϵ_f, mixture $\mathcal{M}_1$ with $T = 500$ K. Reciprocal phase velocity $c/\boldsymbol{v}_\mathrm{p}$ (*left*) and attenuation coefficient $\boldsymbol{\alpha}c/\omega$ (*right*) versus the dimensionless angular frequency ω

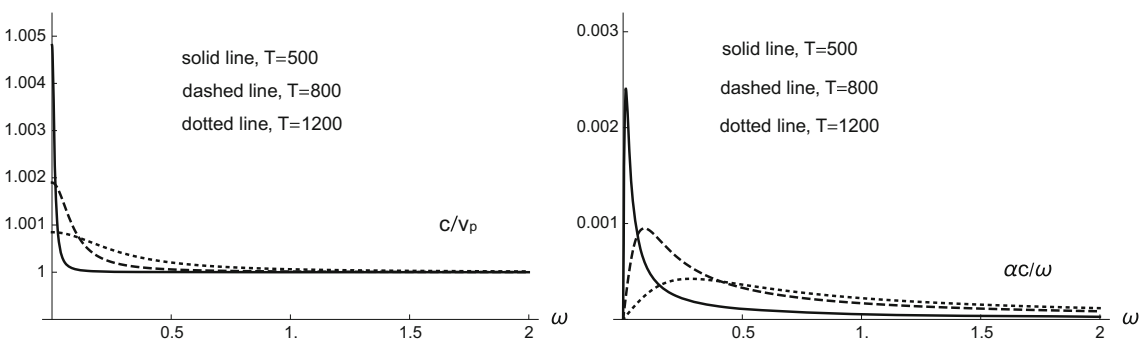

Fig. 2 Influence of the equilibrium temperature T, mixture $\mathcal{M}_2$ with $\epsilon_\mathrm{f} = 23$. Reciprocal phase velocity $c/\boldsymbol{v}_\mathrm{p}$ (*left*) and attenuation coefficient $\boldsymbol{\alpha}c/\omega$ (*right*) versus the dimensionless angular frequency ω

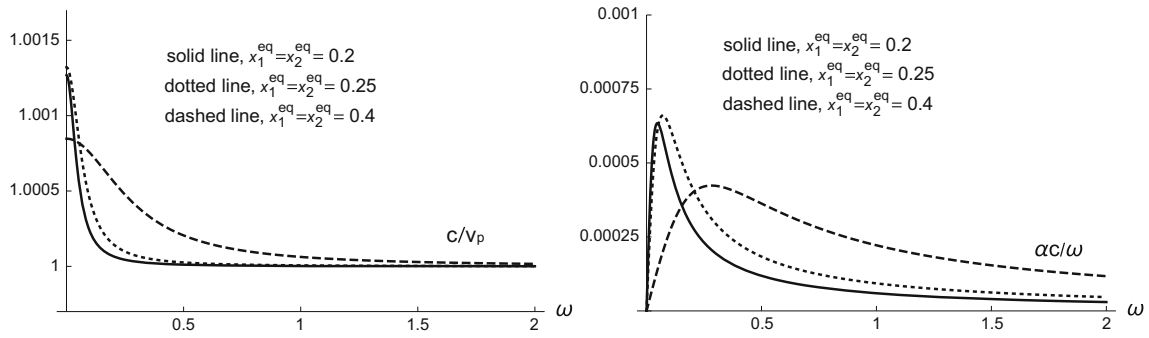

Fig. 3 Different mixtures with different constituent's concentrations. Reciprocal phase velocity $c/\boldsymbol{v}_{\mathrm{p}}$ (*left*) and attenuation coefficient $\boldsymbol{\alpha}c/\omega$ (*right*) versus the dimensionless angular frequency ω

- The effects on the phase velocity and attenuation coefficient just above described can be explained as follows, see [1–3]. A sound wave propagating in a mixture of reactive species in chemical equilibrium causes infinitesimal variations in pressure and temperature that instantaneously induce small non-equilibrium effects in the reactive mixture. The chemical reaction, in turn, drives the mixture toward the chemical equilibrium. However, when the sound wave frequency is very low, the chemical reaction is fast enough to restore the equilibrium very quickly and the effects of the chemical reaction should be visible. On the contrary, when the sound wave frequency is high enough, the chemical composition of the mixture essentially remains the same and the non-equilibrium effects are almost absent so that the impact of the chemical reaction is almost absent. Of course, the trend to equilibrium crucially depends on the activation energy, concentrations and on other chemical kinetic parameters, as evidenced by Figs. 1, 2 and 3.
- In Fig. 1, results on sound propagation are represented for the mixture $\mathcal{M}_1$ at the temperature $T = 500$ K. In this case, the forward chemical reaction is exothermic. Three different values of the forward activation energy are considered, namely $\epsilon_{\mathrm{f}} = 23$ (solid lines), $\epsilon_{\mathrm{f}} = 10$ (dashed lines) and $\epsilon_{\mathrm{f}} = 2.0$ (dotted lines). The exothermicity degree of the reaction is the same in all cases. The solid lines represent the case with higher activation energy, meaning that the threshold of the forward chemical reaction is to high so that only few particles react chemically. In this case, the effects of the chemical reaction are concentrated in the limit $\omega \to 0$, because the chemical reaction rate rapidly approaches to zero, see expressions (13) and (14), and very quickly restores the chemical equilibrium to the reactive mixture. Moreover, as the activation energy decreases, the effects on the phase velocity and attenuation coefficient, as ω increases, become more evident because the chemical reaction is a more frequent process in the evolution of the mixture and the non-equilibrium effects become more significant. However, independently of the value of the activation energy among those considered in Fig. 1, the maximum deviation induced by the chemical reaction (*i.e.,* the peak) on the phase velocity as well as on the attenuation coefficient is the same, namely 7×10^{-3} for the phase velocity and 3.5×10^{-3} for the attenuation coefficient. This is a consequence of a common exothermicity degree for all cases.
- In Fig. 2, we present results on sound propagation for the mixture $\mathcal{M}_2$, considering an activation energy $\epsilon_{\mathrm{f}} = 23$. Three different values of the mixture temperature (in K) are considered, namely $T = 500$ (solid lines), $T = 800$ (dashed lines) and $T = 1200$ (dotted lines). For this mixture, the forward chemical reaction is endothermic and the endothermicity degree of the reaction increases with T, so that the minimum degree of endothermicity corresponds to $T = 500$ (solid lines) and the maximum degree corresponds to $T = 1200$ (dotted lines).
  From the plots in Fig. 2, we observe that the peak of the deviation induced by the chemical reaction is higher for the smaller value of T and lower for the larger value of T. This results from the fact that when the reaction has a larger endothermicity degree (dotted line) the mixture absorbs a larger amount of the energy associated with the passage of the sound waves.
  The plots in Fig. 2 allow also to estimate the effects of the chemical reaction. They show that the maximum deviation induced by the chemical reaction is of order 5×10^{-3} for the phase velocity and 2.3×10^{-3} for the attenuation coefficient, when $T = 500$ K, and of order 1×10^{-3} for the phase velocity and 0.5×10^{-3} for the attenuation coefficient, when $T = 1200$ K.
- Figure 3 illustrates the sound results for the reacting mixtures indicated in Table 1, at the temperature $T = 1200$ K. We consider an activation energy $\epsilon_{\mathrm{f}} = 23$. The forward chemical reaction is endothermic for

the mixture $\mathcal{M}_2$ (dashed line), whereas it is exothermic for the mixtures $\mathcal{M}_1$ (solid line) and $\mathcal{M}_3$ (dotted line), with comparable degrees of exothermicity for mixtures $\mathcal{M}_1$ and $\mathcal{M}_3$. This justifies the fact that mixtures $\mathcal{M}_1$ and $\mathcal{M}_3$ show similar effects on the phase velocity and attenuation coefficient. Additionally, the plots for mixtures $\mathcal{M}_1$ and $\mathcal{M}_3$ evidence a higher peak because the mixture absorbs less energy of the sound waves (exothermic reaction) and the non-equilibrium deviations are more noticeable.

The plots in Fig. 3 show that the maximum deviation induced by the chemical reaction is of order 1.3×10^{-3} for the phase velocity and 6.5×10^{-4} for the attenuation coefficient, for $\mathcal{M}_1$ and $\mathcal{M}_3$, and of order 8×10^{-4} for the phase velocity and 3.5×10^{-4} for the attenuation coefficient, for $\mathcal{M}_2$.

On the other hand, the plots in Fig. 3 show that when $\omega > 0.1$ the effects of the chemical reaction on the phase velocity are more pronounced when the reaction is endothermic, and the same happens when $\omega > 0.2$ for the attenuation coefficient. An analogous behavior has been obtained in paper [5].

6.2 Results for the eigenmodes

In this subsection, we present the results for the dynamics of local wave disturbances appearing in the reactive system described at the beginning of Sect. 6. In detail, we solve numerically the dispersion relation for the considered system and characterize the full spectrum of the eigenmodes.

We obtain six solutions corresponding to three non-propagating eigenmodes (solutions S_1, S_2 and S_3) and three propagating eigenmodes (solutions S_4, S_5 and S_6). Solutions S_5 and S_6 describe hydrodynamic modes, since $\omega(\kappa)$ tends to zero when $\kappa \to 0$, whereas solution S_4 describes a kinetic mode, since $\omega(\kappa)$ tends to a non-vanishing constant value when $\kappa \to 0$. The kinetic mode is clearly associated with the chemical reaction, since it is not present when we turn off the chemical reaction, as it was explained in Sect. 5 when determining the eigenmodes given in (31) for the non-reactive mixture. Moreover, from this analysis, we also realized that solutions S_5 and S_6 have symmetric real parts and the same imaginary part. This indicates that the hydrodynamic modes represent sound waves propagating in opposite directions with the same velocity. Moreover, the kinetic mode is purely diffusive because $Re(S_4) = 0$ in all cases considered here.

The qualitative spectrum obtained in the present work for a chemically reacting quaternary mixture is exactly the same as the one obtained in paper [8] for a binary mixture with chemical reaction. The fact that the mixture is quaternary instead of binary adds two more non-propagating eigenmodes associated with null solutions of the dispersion relation.

Now, we compute explicitly the eigenmodes in the small wavenumber limit and recover the complete spectrum just described above. The results are presented in Figs. 4, 5, 6, 7, 8 and 9, where the longitudinal eigenmodes are plotted with dependence on the dimensionless wavenumber. For convenience, we use the simpler notation ω and κ for the dimensionless frequency $\omega\tau$ and wavenumber $\kappa\ell$.

In order to appreciate the effects of the chemical reaction on the hydrodynamic modes determined by solutions S_5 and S_6, we plot their imaginary parts and the deviations induced on their real parts, say $Re(S_5)+\kappa$ and $Re(S_6)-\kappa$, since in the case of the non-reactive mixture these modes have dimensionless real parts $\pm\kappa$ and vanishing imaginary parts, see expression (31). Furthermore, we also plot the imaginary part of the kinetic mode S_4.

Left diagrams of Figs. 4, 5, 6, 7, 8 and 9 refer to the hydrodynamic modes, while right diagrams refer to the kinetic mode. In the left diagrams, we show the deviations induced on the real parts of the angular frequency ω, i.e., on the oscillation frequency of the wave disturbances. We also show the imaginary parts of the angular frequency ω, which represents the time decay of the oscillation amplitude of the wave disturbances. In the right diagrams, we show the imaginary part of the angular frequency ω, only, since the real part vanishes, as explained before.

- Figures 4, 5 and 6 refer to the mixture $\mathcal{M}_1$ for which the forward chemical reaction is exothermic, whereas Figs. 7, 8 and 9 refer to the mixture $\mathcal{M}_2$ for which the forward chemical reaction is endothermic. With the exceptions of the cases represented in Figs. 6 and 9 for $\epsilon_f = 23$ and in Figs. 4 and 7 for $T = 500$ K, in all study cases we have considered a low activation energy and a high value of the temperature, $\epsilon_f = 2$ and $T = 1200$ K, in order to better appreciate the effects of the chemical reaction. Figures with $\epsilon_f = 23$ or $T = 500$ K are important when analyzing the influence of the activation energy and of the temperature.
- Let us comment first on the qualitative aspects recognizable in all figures for the eigenmodes associated with solutions S_4, S_5, S_6. All modes show a stable behavior (in time) because the imaginary part of the solutions is negative, see also expressions (22). All figures show that the hydrodynamic modes S_5, S_6

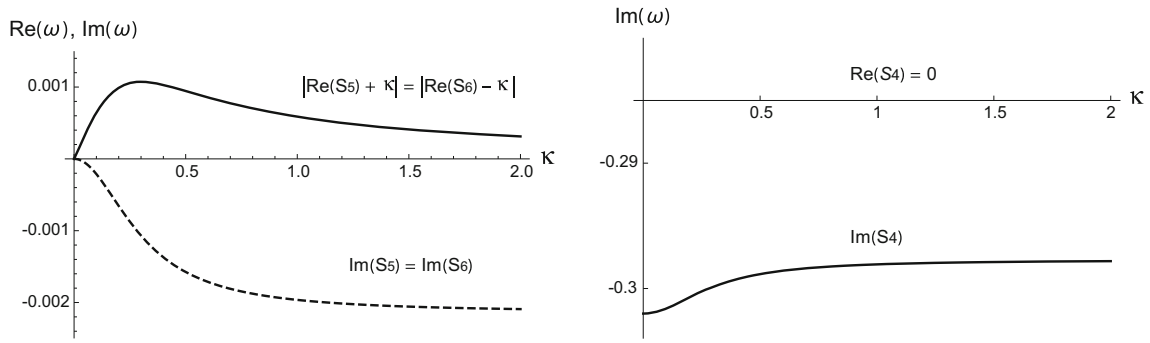

Fig. 4 Longitudinal eigenmodes as functions of the wavenumber κ for the mixture $\mathcal{M}_1$, exothermic reaction with $T = 500$ K, $\epsilon_f = 2$. Representation of the hydrodynamic modes (*left*) and of the kinetic mode (*right*)

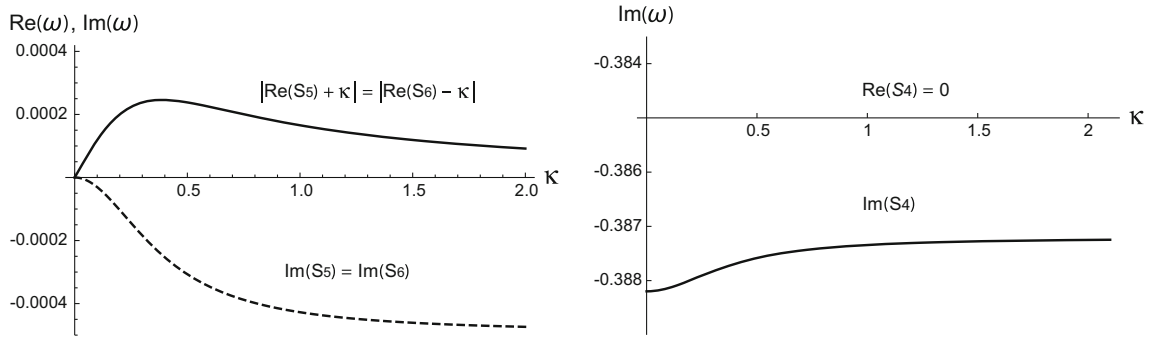

Fig. 5 Longitudinal eigenmodes as functions of the wavenumber κ for the mixture $\mathcal{M}_1$, exothermic reaction with $T = 1200$ K, $\epsilon_f = 2$. Representation of the hydrodynamic modes (*left*) and of the kinetic mode (*right*)

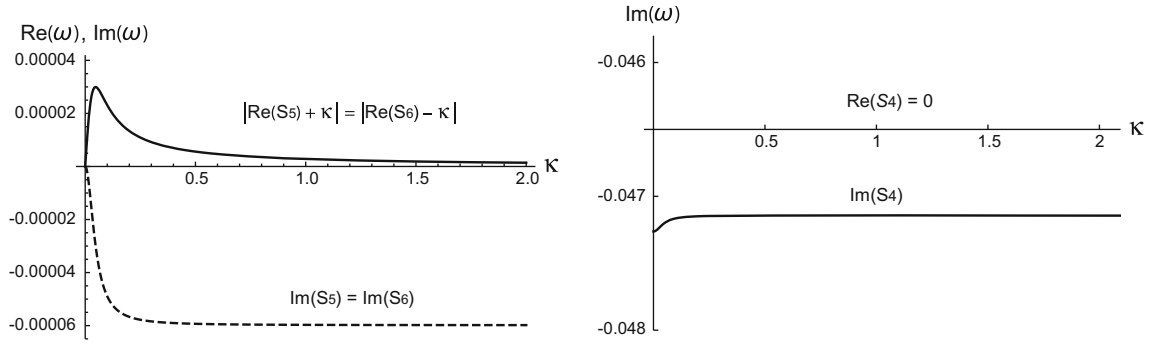

Fig. 6 Longitudinal eigenmodes as functions of the wavenumber κ for the mixture $\mathcal{M}_1$, exothermic reaction with $T = 1200$ K, $\epsilon_f = 23$. Representation of the hydrodynamic modes (*left*) and of the kinetic mode (*right*)

describe sound waves propagating in opposite direction. In fact, we can see that S_5, S_6 have symmetric real parts (and thus opposite velocities) and the same imaginary part (and thus the same damping). All figures also show that the kinetic mode S_4 is always purely non-propagating diffusive, since its real part is zero and its imaginary part is negative. Moreover, in all cases, the damping of the kinetic mode is more pronounced than that of the hydrodynamic modes.

- Now, in order to appreciate in detail the effects of the chemical reaction on the eigenmodes, let us compare the different plots.
  - Comparing first Figs. 5 and 6 for mixture $\mathcal{M}_1$, exothermic reaction, $T = 1200$ K, or Figs. 8 and 9 for mixture $\mathcal{M}_2$, endothermic reaction, $T = 1200$ K, we can appreciate the effects of the activation energy on the eigenmodes. We clearly observe that, as expected, the effects are more noticeable in Figs. 5 and 8 when $\epsilon_f = 2$, than in Figs. 6 and 9 when $\epsilon_f = 23$. In particular, we observe that when $\epsilon_f = 2$ and the chemical reaction is more frequent, a larger deviation on the real parts of the hydrodynamic modes with

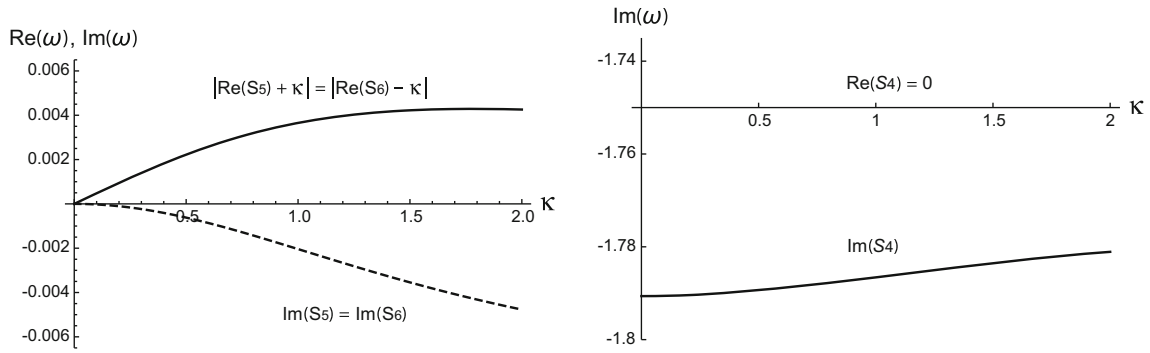

Fig. 7 Longitudinal eigenmodes as functions of the wavenumber κ for the mixture $\mathcal{M}_2$, endothermic reaction with $T = 500$ K, $\epsilon_f = 2$. Representation of the hydrodynamic modes (*left*) and of the kinetic mode (*right*)

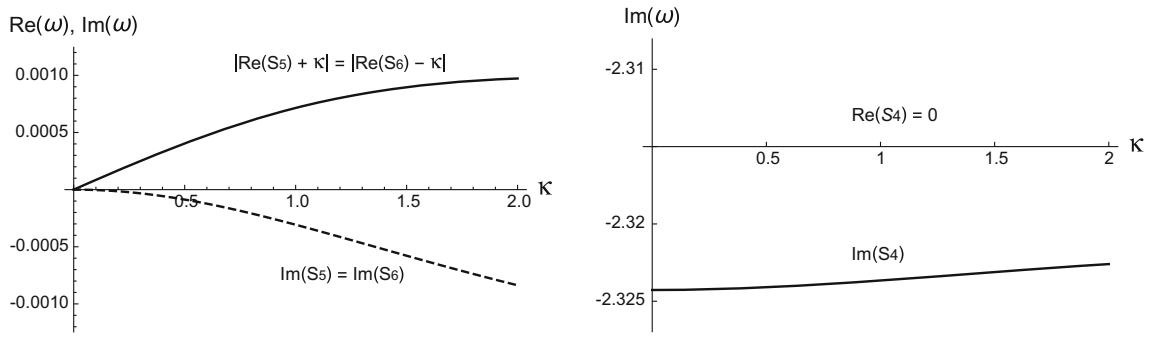

Fig. 8 Longitudinal eigenmodes as functions of the wavenumber κ for the mixture $\mathcal{M}_2$, endothermic reaction with $T = 1200$ K, $\epsilon_f = 2$. Representation of the hydrodynamic modes (*left*) and of the kinetic mode (*right*)

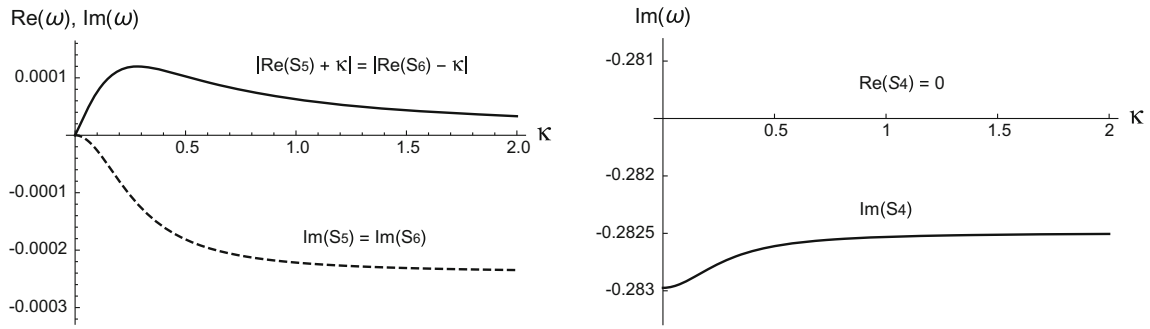

Fig. 9 Longitudinal eigenmodes as functions of the wavenumber κ for the mixture $\mathcal{M}_2$, endothermic reaction with $T = 1200$ K, $\epsilon_f = 23$. Representation of the hydrodynamic modes (*left*) and of the kinetic mode (*right*)

respect to $\pm\kappa$ is observed. Additionally, the amplitude decay (imaginary parts) of the kinetic and of the hydrodynamic modes increases. The behavior through this comparison is justified by the fact that the influence of the chemical reaction is more evident when the energy barrier imposed by the activation energy is low and more collisions with chemical reaction are occurring.

– Comparing now Figs. 4 and 7 for $T = 500$ K, $\epsilon_f = 2$, or Figs. 5 and 8 for $T = 1200$ K, $\epsilon_f = 2$, we can appreciate the effects of the exothermicity/endothermicity on the eigenmodes. We can observe that the qualitative behavior of the solutions is the same when the forward reaction is exothermic or endothermic. However, the effects of the chemical reaction are more pronounced when the chemical reaction is endothermic (Figs. 7, 8), in the sense that both the deviation of the oscillation frequency (real parts) and the amplitude decay (imaginary parts) are larger when the reaction is endothermic.
– Finally, comparing Figs. 4 and 5 for mixture $\mathcal{M}_1$, exothermic reaction, $\epsilon_f = 2$, or Figs. 7 and 8 for mixture $\mathcal{M}_2$, endothermic reaction, $\epsilon_f = 2$, , we can appreciate the effects of the temperature on the eigenmodes. We observe that when the temperature is high the deviation of the oscillation frequency

(real part) of the hydrodynamic modes decreases. The amplitude decay (imaginary part) of the kinetic mode increases, whereas the one of the hydrodynamic modes decreases. This behavior indicates that when the temperature is high the effects of the chemical reaction are more pronounced in the kinetic mode and less evident in the hydrodynamic modes.

7 Concluding remarks

Our analysis developed in this paper, based on the reactive Euler equations for a quaternary mixture, was able to capture some effects of the chemical reaction on the sound propagation as well as on the propagation of local wave disturbances appearing in the reactive system. Naturally, the analysis presents some limitations but also some interesting points, and we will comment on both.

We start by mentioning two significant limitations. First, we were not able to test the agreement of the model with experimental observations, because we did not find available data to implement the comparison with real physical systems. Second, we have used an idealized model for monatomic mixtures to mimic a realistic chemical reaction occurring in polyatomic mixtures. These represent perhaps the stronger limitations of our study.

Now we comment on the positive aspects of the study. The mathematical model incorporates some relevant elements for an appropriate description of the problems studied here within reactive mixtures. In particular, the numerical tests implemented in the paper provide valuable information about the effects of the chemical reaction on the properties of interest in the propagating problems. Another important aspect of our analysis is the fact that the reactive source terms appearing in the model equations have been explicitly computed from the kinetic theory. Thus, they show a detailed dependence on some key parameters in the reactive process, namely the heat of the chemical reaction, the activation energy of the forward reaction and the concentrations of the constituents.

Therefore, regardless of the limitations, we believe that our study offers some insights into the chemical kinetics of forced and free waves and can be useful to develop better mathematical models and conduct other computational or even experimental studies on these topics.

Some possible improvements to the preliminary investigation carried out in this paper should be oriented following two different lines of investigation.

(a) A first line should be developed in order to investigate the high-frequency limit of sound propagation in a chemically reactive mixture, using the method proposed in [10] for one component gas.
(b) A second line, but apparently more difficult, should be developed in order to deepen the effects of the chemical reaction by considering a model for polyatomic gases, since reactive mixtures are, in general, polyatomic systems. In particular, Refs. [19,20] and [21,22] propose mathematical models to describe polyatomic systems, respectively, with and without chemical reaction. Therefore, the literature concerning wave propagation within non-reactive polyatomic gases, and we quote for example Refs. [13,15,23], should be enriched with further studies when chemical reactions are involved.

Acknowledgements The paper is partially supported by the Research Centre of Mathematics of the University of Minho, with the Portuguese Funds from the Foundation for Science and Technology (FCT) through the Project UID/MAT/00013/2013. We wish to thank the anonymous Referees for their valuable comments and suggestions that helped us to improve the paper.

Appendix

In this appendix, we give the details of the calculations for the components of the first line of the matrix $\left(\mathbf{H}_{\alpha\beta}\right) = \left(\frac{\partial \mathbf{S}}{\partial \mathbf{U}}\right)_0$ presented in expressions (20) of Sect. 3, with $\mathbf{S}$ and $\mathbf{U}$ being the vectors of the source contributions and mixture fields, respectively, introduced in Eq. (11).

Each source term τ_α is a function of the fields $\varrho_1, \ldots, \varrho_4$ and of the mixture temperature T, see (13), which is not a field in our theory. The temperature T, in turn, is a function of all fields $\varrho_1, \ldots, \varrho_4, \varrho v, \varrho e$, whose functional dependence can be obtained from Eqs. (7) and (2) in the form

$$T = \frac{1}{\varrho c_{\mathrm{v}}}\left[\varrho e - \frac{1}{2\varrho}(\varrho v)^2 - \sum_{\alpha=1}^{4} \varrho_\alpha \frac{\epsilon_\alpha}{m_\alpha}\right]. \tag{34}$$

Therefore, the elements of the matrix $\left(\mathbf{H}_{\alpha\beta}\right)$ were calculated using the chain rule.

(a) In the case of $\mathbf{H}_{11}$ the chain rule gives

$$\mathbf{H}_{11} = \left(\frac{\partial \tau_1}{\partial \varrho_1} + \frac{\partial \tau_1}{\partial T}\frac{\partial T}{\partial \varrho_1}\right)_0 \tag{35}$$

where

$$\frac{\partial \tau_1}{\partial \varrho_1} = -\sqrt{\frac{8\pi kT}{m_{12}}} d_{\mathrm{f}}^2 \exp\left(-\frac{\epsilon_{\mathrm{f}}}{kT}\right) n_2, \tag{36}$$

$$\frac{\partial \tau_1}{\partial T} = \frac{m_1}{2T}\tau_1 + m_1\sqrt{\frac{8\pi}{kT^3}}\left[\frac{n_3 n_4}{\sqrt{m_{34}}}\epsilon_{\mathrm{r}} d_{\mathrm{r}}^2 \exp\left(-\frac{\epsilon_{\mathrm{r}}}{kT}\right) - \frac{n_1 n_2}{\sqrt{m_{12}}}\epsilon_{\mathrm{f}} d_{\mathrm{f}}^2 \exp\left(-\frac{\epsilon_{\mathrm{f}}}{kT}\right)\right], \tag{37}$$

$$\frac{\partial T}{\partial \varrho_1} = \frac{1}{\varrho c_{\mathrm{v}}}\left[-\frac{\epsilon_1}{m_1} + \frac{1}{2\varrho^2}(\varrho v)^2\right] - \frac{T}{\varrho}\,. \tag{38}$$

At equilibrium, the momentum ϱv and the reaction rate τ_1 vanish, so that substituting expressions (36), (37) and (38) referred to equilibrium into (35), we obtain

$$\mathbf{H}_{11} = -\left\{\sqrt{\frac{8\pi kT}{m_{12}}} \exp\left(-\frac{\epsilon_{\mathrm{f}}}{kT}\right) d_{\mathrm{f}}^2 n_2 \left[1 + \frac{\varrho_1}{kT^2}\left(\frac{T}{\varrho} + \frac{1}{\varrho c_{\mathrm{v}}}\frac{\epsilon_1}{m_1}\right)(\epsilon_{\mathrm{r}} - \epsilon_{\mathrm{f}})\right]\right\}_0 .$$

Introducing the concentrations $x_\alpha^{\mathrm{eq}} = n_\alpha^{\mathrm{eq}}/n$, the dimensionless reaction rate Q^*, as well as the reference time τ and the Arrhenius factor Δ together with the formula $d_{\mathrm{f}} = d_{12}s_{\mathrm{f}}$, into the expression for $\mathbf{H}_{11}$ presented above, gives

$$\mathbf{H}_{11} = -\frac{\Delta}{\tau x_1^{\mathrm{eq}}} + m_1\left(\frac{n}{\varrho} + \frac{2}{3m_1}\frac{\epsilon_1}{kT}\right) Q^*\frac{\Delta}{\tau}\,.$$

(b) In a similar fashion, we apply the chain rule to obtain

$$\mathbf{H}_{12} = \left(\frac{\partial \tau_1}{\partial \varrho_2} + \frac{\partial \tau_1}{\partial T}\frac{\partial T}{\partial \varrho_2}\right)_0,$$

where $\frac{\partial \tau_1}{\partial T}$ is given by Eq. (37) and

$$\frac{\partial \tau_1}{\partial \varrho_2} = -\frac{m_1}{m_2}\sqrt{\frac{8\pi kT}{m_{12}}} d_{\mathrm{f}}^2 \exp\left(-\frac{\epsilon_{\mathrm{f}}}{kT}\right) n_1,$$

$$\frac{\partial T}{\partial \varrho_2} = \frac{1}{\varrho c_{\mathrm{v}}}\left[-\frac{\epsilon_2}{m_2} + \frac{1}{2\varrho^2}(\varrho v)^2\right] - \frac{T}{\varrho}\,.$$

At equilibrium, we obtain

$$\mathbf{H}_{12} = -\left\{\sqrt{\frac{8\pi kT}{m_{12}}} \exp\left(-\frac{\epsilon_{\mathrm{f}}}{kT}\right) d_{\mathrm{f}}^2 \frac{\varrho_1}{m_2}\left[1 + \frac{\varrho_2}{kT^2}\left(\frac{T}{\varrho} + \frac{1}{\varrho c_{\mathrm{v}}}\frac{\epsilon_2}{m_2}\right)(\epsilon_{\mathrm{r}} - \epsilon_{\mathrm{f}})\right]\right\}_0$$

or, in dimensional form,

$$\mathbf{H}_{12} = -\frac{m_1}{m_2}\frac{\Delta}{\tau x_2^{\mathrm{eq}}} + m_1\left(\frac{n}{\varrho} + \frac{2}{3m_2}\frac{\epsilon_2}{kT}\right) Q^*\frac{\Delta}{\tau}.$$

(c) Analogously, for $\mathbf{H}_{13}$, we obtain

$$\mathbf{H}_{13} = \left\{ \sqrt{\frac{8\pi kT}{m_{12}}}\, \exp\left(-\frac{\epsilon_\mathrm{f}}{kT}\right) d_\mathrm{f}^2\, n_2\, \frac{\varrho_1}{\varrho_3} \left[1 - \frac{\varrho_3}{kT^2} \left(\frac{T}{\varrho} + \frac{1}{\varrho c_\mathrm{v}} \frac{\epsilon_3}{m_3} \right) (\epsilon_\mathrm{r} - \epsilon_\mathrm{f}) \right] \right\}_0$$

or, in dimensional form,

$$\mathbf{H}_{13} = \frac{m_1}{m_3} \frac{\Delta}{\tau x_3^{\mathrm{eq}}} + m_1 \left(\frac{n}{\varrho} + \frac{2}{3m_3} \frac{\epsilon_3}{kT} \right) Q^* \frac{\Delta}{\tau}\,.$$

(d) For $\mathbf{H}_{14}$, we obtain

$$\mathbf{H}_{14} = \left\{ \sqrt{\frac{8\pi kT}{m_{12}}}\, \exp\left(-\frac{\epsilon_\mathrm{f}}{kT}\right) d_\mathrm{f}^2\, n_2\, \frac{\varrho_1}{\varrho_4} \left[1 - \frac{\varrho_4}{kT^2} \left(\frac{T}{\varrho} + \frac{1}{\varrho c_\mathrm{v}} \frac{\epsilon_4}{m_4} \right) (\epsilon_\mathrm{r} - \epsilon_\mathrm{f}) \right] \right\}_0$$

or, in dimensional form,

$$\mathbf{H}_{14} = \frac{m_1}{m_4} \frac{\Delta}{\tau x_4^{\mathrm{eq}}} + m_1 \left(\frac{n}{\varrho} + \frac{2}{3m_4} \frac{\epsilon_4}{kT} \right) Q^* \frac{\Delta}{\tau}\,.$$

(e) For the component $\mathbf{H}_{15}$, the chain rule gives

$$\mathbf{H}_{15} = \left(\frac{\partial \tau_1}{\partial T}\, \frac{\partial T}{\partial(\varrho v)} \right)_0,$$

where

$$\frac{\partial T}{\partial(\varrho v)} = -\frac{v}{\varrho c_\mathrm{v}}$$

which vanishes in equilibrium, and therefore $\mathbf{H}_{15} = 0$.

(f) Finally, for the component $\mathbf{H}_{16}$, the chain rule gives

$$\mathbf{H}_{16} = \left(\frac{\partial \tau_1}{\partial T}\, \frac{\partial T}{\partial(\varrho e)} \right)_0,$$

where

$$\frac{\partial T}{\partial(\varrho e)} = \frac{1}{\varrho c_\mathrm{v}}.$$

Therefore

$$\mathbf{H}_{16} = \left[\sqrt{\frac{8\pi}{kT^3 m_{12}}}\, \frac{1}{\varrho c_\mathrm{v}} \exp\left(-\frac{\epsilon_\mathrm{f}}{kT}\right) d_\mathrm{f}^2 \varrho_1 \frac{\varrho_2}{m_2}\, (\epsilon_\mathrm{r} - \epsilon_\mathrm{f}) \right]_0.$$

or, in dimensional form,

$$\mathbf{H}_{16} = -\frac{2}{3} \frac{m_1}{kT} Q^* \frac{\Delta}{\tau}\,.$$

References

1. Barton, J.P.: Sound propagation within a chemically reacting ideal gas. J. Acoust. Soc. Am. **81**, 233–237 (1987)
2. Haque, M.Z.: Effects of chemical kinetics on sound propagation within high temperature hydrocarbon combustion products. Ph.D. Thesis, University of Nebraska-Lincoln (1996)
3. Haque, M.Z., Barton, J.P.: A theoretical tool to predict the effects of chemical kinetics on sound propagation within high temperature hydrocarbon combustion products. In: ASME Proceedings of International Gas Turbine Aeroengine Congress and Exhibition, Vol. 2, Paper No. 99-GT-276, pp. 1–6 (1999)
4. Garcia-Colin, L.S., de la Selva, S.M.Y.: On the propagation of sound in chemically reacting fluids. Physica **75**, 37–56 (1974)
5. Marques Jr., W., Alves, G.M., Kremer, G.M.: Light scattering and sound propagation in a chemically reacting binary gas mixture. Phys. A **323**, 401–412 (2003)
6. Kremer, G.M., Pandolfi Bianchi, M., Soares, A.J.: A relaxation kinetic model for transport phenomena in a reactive flow. Phys. Fluids **18**(037104), 1–15 (2006)
7. Alves, G.M., Kremer, G.M., Marques Jr., W., Soares, A.J.: A kinetic model for chemical reactions without barriers: transport coefficients and eigenmodes. J. Stat. Mech. **P03014**, 1–20 (2011)
8. Marques Jr., W., Kremer, G.M., Soares, A.J.: Influence of reaction heat on time dependent processes in a chemically reacting binary mixture. In: 28th International Symposium on Rarefied Gas Dynamics 2012. AIP Conference Proceedings, Vol. 1501, pp. 137–144 (2012)
9. Kremer, G.M.: An introduction to the Boltzmann equation and transport processes in gases. Springer, Berlin (2010)
10. Muracchini, A., Ruggeri, T., Seccia, L.: Dispersion relation in the high frequency limit and non linear wave stability for hyperbolic dissipative systems. Wave Motion **15**, 143–158 (1992)
11. Fernandes, A.S., Marques Jr., W.: Sound propagation in binary gas mixtures from a kinetic model of the Boltzmann equation. Phys. A **332**, 29–46 (2004)
12. Fernandes, A.S., Marques Jr., W.: Free wave propagation in binary gas mixtures. Contin. Mech. Thermodyn. **17**, 297–307 (2005)
13. Fernandes, A.S., Marques Jr., W.: Kinetic model analysis of time-dependent problems in polyatomic gases. Phys. A **373**, 97–118 (2007)
14. Napier, D.G., Shizgal, B.D.: Sound dispersion in single-component systems. Phys. A **387**, 4099–4118 (2008)
15. Arima, T., Taniguchi, S., Ruggeri, T., Sugiyama, M.: Dispersion relation for sound in rarefied polyatomic gases based on extended thermodynamics. Contin. Mech. Thermodyn. **25**, 727–737 (2013)
16. Kalempa, D., Sharipov, F.: Sound propagation through a binary mixture of rarefied gases at arbitrary sound frequency. Eur. J. Mech. B Fluids **57**, 50–63 (2016)
17. Kremer, G.M., Marques Jr., W.: Fourteen moment theory for granular gases. KRM **4**, 317–331 (2011)
18. Kremer, G.M., Marques Jr., W.: Analysis of eigenmodes in a relativistic gas. Contin. Mech. Thermodyn. **24**, 719–729 (2012)
19. Desvillettes, L., Monaco, R., Salvarani, F.: A kinetic model allowing to obtain the energy law of polytropic gases in the presence of chemical reactions. Eur. J. Mech. B Fluids **24**, 219–236 (2005)
20. Bisi, M., Spiga, G.: On kinetic models for polyatomic gases and their hydrodynamic limits. Ric. Mat. doi:10.1007/s11587-016-0289-5 **(in press)**
21. Arima, T., Taniguchi, S., Ruggeri, T., Sugiyama, M.: Extended thermodynamics of dense gases. Contin. Mech. Thermodyn. **24**, 271–292 (2012)
22. Pavić, M., Ruggeri, T., Simić, S.: Maximum entropy principle for rarefied polyatomic gases. Phys. A **392**, 1302–1317 (2013)
23. Arima, T., Taniguchi, S., Ruggeri, T., Sugiyama, M.: A study of linear waves based on extended thermodynamics for rarefied polyatomic gases. Acta Appl. Math. **132**, 15–25 (2014)